Published in final edited form as:
Cryst Growth Des. 2008 August ; 8(8): 3084–3090. doi:10.1021/cg800252f.

Bio-inspired Synthesis of Mineralized Collagen Fibrils

Atul S. Deshpande and **Elia Beniash***
Dept Oral Biology, Center for Craniofacial Regeneration, University of Pittsburgh School of Dental Medicine, Dept of Bioengineering, University of Pittsburgh School of Engineering, McGowan Institute for Regenerative Medicine, Pittsburgh, PA, USA

Abstract

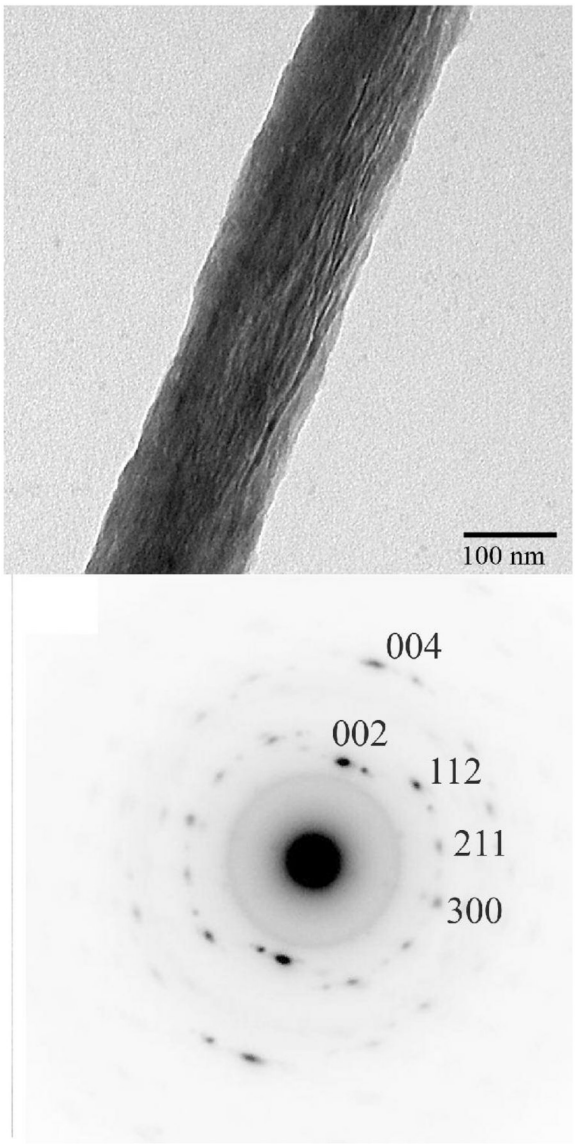

*Corresponding Author: Elia Beniash, PhD, Associate Professor, Oral Biology, University of Pittsburgh School of Dental Medicine, McGowan Institute for Regenerative Medicine, 589 Salk Hall, 3501 Terrace Street, Pittsburgh, PA 15261, USA, Tel. 412 6480108, Fax 412 6246685, Email: ebeniash@pitt.edu.

Mineralized collagen fibrils constitute a basic structural unit of collagenous mineralized tissues such as dentin and bone. Understanding of the mechanisms of collagen mineralization is vital for development of new materials for the hard tissue repair. We carried out bio-inspired mineralization of reconstituted collagen fibrils using poly-l-aspartic acid, as an analog of non-collagenous acidic proteins. Transmission electron microscopy and electron diffraction studies of the reaction products revealed stacks of ribbon-shaped apatitic crystals, deposited within the fibrils with their *c*-axes co-aligned with the fibril axes. Such structural organization closely resembles mineralized collagen of bone and dentin. Initial mineral deposits formed in the fibrils lacked a long range crystallographic order and transformed into crystals with time. Interestingly, the shape and organization of these amorphous deposits was similar to the crystals found in the mature mineralized fibrils. We demonstrate that the interactions between collagen and poly-l-aspartic acid are essential for the mineralized collagen fibrils formation, while collagen alone does not affect mineral formation and poly-l-aspartic acid inhibits mineralization in a concentration dependant manner. These results provide new insights into basic mechanisms of collagen mineralization and can lead to the development of novel bio-inspired nanostructured materials.

Keywords

Biomineralization; Amorphous Calcium Phosphate; Nanocomposite; TEM; Hydroxyapatite

Introduction

Understanding of the basic strategies of biomineralization of collagenous mineralized tissues (CMTs), such as bone and dentin, is essential for the development of novel bio-inspired materials for hard tissue repair and regeneration. CMTs are organo-mineral composite materials with high structural and compositional complexity. They are organized into several hierarchical levels, beginning at the the nanoscale [1]. The basic building block of CMTs is a mineralized collagen fibril containing plate-shaped carbonated apatite crystals oriented with their *c*-axis along the long axis of the fibril [2–5]. The differences between different types of bone and dentin are largely determined by variations in the organization of mineralized collagen fibrils as well as the extent of their mineralization [1]. Formation of biominerals, including CMTs, is a multi-step process involving secretion of extracellular matrix (ECM) and controlled deposition of mineral phase [6, 7]. It is widely accepted that biomacromolecules regulate many aspects of mineral formation, including control of the phase, orientation, shape and organization of mineral deposits in mineralized tissues [8, 9].

Although collagen comprises more than 90% of total organic matrix of CMTs there are dozens of other proteins present in small amounts in these tissues [10–12]. These, so called non-collagenous proteins, are believed to play essential roles in the formation of CMTs. One of the common characteristics of these non-collagenous proteins is the high content of acidic amino acids such as aspartate (D), glutamate (E) and phosphoserine ($S^{(P)}$). For example, 77% of phosphophoryn, the major non-collagenous dentin protein, is comprised of SSD repetitive motif, with 70 to 80% of serines phosphorylated. *In vitro* studies demonstrate that acidic non-collagenous proteins in CMTs can regulate crystal nucleation, control crystal shape, inhibit mineralization and stabilize metastable mineral phases [10, 13–15]. Interestingly, many of these molecules can have different and sometimes opposite effects on mineralization, depending on the parameters of the mineralization system, such as the protein concentration and either the protein is in solution or in a bound state [10]. Several knockouts of the non-collagenous proteins were reported in the literature. Although the absence of a single non-collagenous protein in many cases induced changes in bones and dentin of various severity none of these knockouts lead to a complete cessation of collagen mineralization, suggesting that there is a redundancy in the functions of non-collagenous proteins in CMTs [16–19].

Over the last two decades stabilized amorphous phases that transform into crystals were detected in a numerous biomineralization systems, suggesting that such biomineralization mechanism can be more widespread than previously thought [20–25]. There is a number of reports suggesting that the first mineral formed in CMTs is amorphous calcium phosphate (ACP) [24, 26, 27]. In particular, ACP has been shown to form in matrix vesicles and trigger collagen mineralization [28–31]. Despite these numerous studies there is still an ongoing debate around the idea of amorphous precursors in the CMT formation. This is in part due to the technical difficulties of the proper identification and analysis of ACP, which often leads to ambiguous results.

As evident from the preceding paragraphs, biomineralization of CMTs is a complex process, which is extremely difficult to study *in vivo*. *In vitro* collagen mineralization experiments, which closely simulate biological conditions, can provide new insights into basic processes of CMT formation and lead to the development of new bio-inspired nanostructured materials for hard tissue repair and regeneration. Since the mineralized collagen fibril is the basic structural and functional element of the CMTs the ability to recreate it *in vitro* is essential for development of nanostructured bio-inspired materials for mineralized tissue repair. A number of experimental attempts to recreate the mineralized collagen fibrils *in vitro* have been reported over the last decade. Bradt et. al. [32] carried out mineralization of collagen fibrils in the presence of poly-l-aspartic acid (polyAsp) involving simultaneous assembly of collagen fibrils and calcium phosphate precipitation. The needle shaped crystals formed in these experiments, although attached to collagen fibrils, did not show any specific orientation with respect to collagen fibers. Later, Zhang et. al. [33] used a similar methodology but without the use of polyAsp, resulting in the deposition of hydroxyapatite crystals on the collagen fibrils, oriented along the fibril axis. Very recently Olszta et. al [34] reported mineralization of collagen fibrils via homogeneous precipitation of amorphous calcium phosphate from highly supersaturated solution followed by polyAsp induced crystallization. The final product of this reaction was a mineralized collagen fibril with the crystalline *c*-axes oriented along the axis of the fibril. Though these reports show promising results, the experimental approaches developed in these studies differ significantly from the biological mineralization process.

Here, we report mineralization of type-I collagen fibrils deposited as a single layer on carbon coated TEM grids in the presence of polyAsp, used as a model of acidic non-collagenous proteins. The deposition of collagen fibrils in a single layer vs. bulk gel or suspension allows one to overcome problems of diffusion gradients of mineral ions and minimizes sample preparation steps for TEM analysis. Our mineralization experiments were designed to reproduce as close as possible the physiological physico-chemical conditions and achieve a high level of control of the mineralization kinetics. We anticipate that the results of our experiments will lead to the better understanding of collagen mineralization processes.

Experimental Section

Preparation of purified collagen solution

Acidic solution of type I collagen was obtained from rat tail tendon. The tendons were collected from 4–8 weeks old rats and washed in protease inhibitor buffer [35] Then the tendons were briefly rinsed in deionized water, homogenized and solubilized in 2mM HCl (pH 2.8). The collagen solution was centrifuged at 25000×g to remove aggregates. Collagen was then purified by several cycles of selective salt precipitation followed by acid dissolution as reported elsewhere [35–37]. The purity of the isolated collagen was tested by SDS-PAGE electrophoresis.

Stock solutions

High purity $CaCl_2 \cdot 2H_2O$, $(NH_4)_2HPO_4$ and polyAsp (5000–15000 $gmol^{-1}$) were obtained from Sigma-Aldrich. A 10X PBS buffer with 100 mM sodium phosphate and 1550 mM NaCl was purchased from Fluka. Stock solutions of $CaCl_2$ (6.68 mM), $(NH_4)_2HPO_4$ (4 mM) and polyAsp (500–15.625 μgml^{-1}) were prepared using deionized distilled water (DDW) with the resistivity of 18.2 MΩ*cm.

Self-assembly of collagen fibrils

Typically, 90 µl of acidic collagen solution and 10 µl of 10X PBS solution were mixed together to obtain 0.1–0.2% collagen solution in 1X PBS. Twenty µl droplet of this mixed solution was placed on a inert polyethylene substrate in a humidity chamber and a carbon coated Ni grid (EMS, Hatfield, PA) was placed on top of the droplet. The humidity chamber was sealed and the sample was incubated at 37 °C for 3h. After the incubation, the grid was quickly washed with DDW and blotted against a filter paper and air dried. For TEM analysis of self assembled collagen fibrils the samples were positively stained with 1% uranyl acetate solution for 30 min.

Mineralization Experiments

In our mineralization experiments we attempted to reproduce, as close as possible, the conditions found during the mineralized tissue formation. There are only few studies that provide information about the mother liquid composition in the mineralization environment [38, 39]. In general their inorganic chemical composition is similar to other body fluids with exception for the elevated phosphate content. For example, in enamel fluid phosphate content is ~4 mM. We therefore decided to use PBS with 1.67 mM $CaCl_2$ as a basic medium for the mineralization reaction. During our preliminary studies we have found that 4 mM PBS had insufficient buffer capacity to keep the pH of the reaction constant, which lead to inadequate reproducibility of the results. *In vivo* the pH of the mineralization compartment is tightly regulated, as shown in the studies of enamel formation [40]. This is achieved by a function of enzymes, such as carbonic anhydrases, proton pumps and ion channels. In order to minimize the pH change in the *in vitro* system we have increased the concentration of the phosphate. After a series of preliminary studies we have empirically found that reproducible results can be achieved at the phosphate concentrations of 9.5 mM. We therefore used this concentration in our mineralization studies.

Control mineralization

For the control mineralization experiments, x3.4 PBS was prepared from x10 PBS stock solution. The pH of x10 PBS solution was adjusted to give pH 7.7, when diluted 10 times. Five µl of x3.4 PBS was mixed with 5 µl of DDW, 5 µl of 4 mM $(NH_4)_2HPO_4$ and 5 µl of 6.8 mM $CaCl_2$ stock solutions to achieve final concentrations of 1.67mM $CaCl_2$, 1mM $(NH_4)_2HPO_4$ and 0.85X PBS (8.5 mM phosphate, 131.7 mM NaCl). Droplets of mineralization solution were placed in a humidity chamber and carbon coated Ni grids (#400) (EMS, Hatfield, PA) were placed on the top of the droplets. The chamber was sealed and was kept at 37°C for 6 hours. After the incubation the TEM grids were quickly rinsed with DDW, blotted against a filter paper and air dried.

Mineralization experiments with polyAsp

The experiments were performed as described in the previous paragraph; however 5 µL pf polyAsp solution was added to the mineralization medium instead of DDW. The final concentration of polyAsp varied from 125 µg/ml to 3.90 µg/ml.

Collagen mineralization in the absence of polyAsp

The mineralization reaction has been performed as in control mineralization experiments. It has been carried out on the grids coated with collagen fibrils as described in the section on the self-assembly of collagen fibrils.

Collagen mineralization in the presence of polyAsp

Collagen mineralization has been performed as described in the section above, however polyAsp has been added to the mineralization solution to the final concentration of 62.5 μg/ml. The grids were incubated for 2 to 16 hours in the humidity chamber at 37 °C.

Transmission Electron Microscopy (TEM) and Selected Area Electron Diffraction (SAED) analysis

Transmission electron microscopy (TEM) and selected area electron diffraction (SAED) studies were carried out using JEOL 1200 EX and JEOL 1210 TEM microscopes at 100 kV. The micrographs were recorded using AMT CCD camera (AMT, Danvers, MA). An aluminum film coated TEM grid (EMS Hatfield, PA) was used as a standard to calibrate SAED patterns for d-spacing calculations. The micrographs were analyzed using ImageJ 1.38x image processing software (Bethesda, MD).

Results and Discussion

Collagen self-assembly

The self-assembly of collagen fibrils was carried out in PBS at 37 °C as described in the Materials and Methods section. The TEM analysis of positively stained samples revealed that the reconstituted fibrils were several microns long, 119 nm (SD ± 59) wide and had a typical banding pattern with ~67 nm periodicity, characteristic of native collagen assembly [41] (Figure 1).

Control mineralization experiments on the bare carbon coated TEM grids

Control mineralization experiments carried out in PBS on bare TEM grids without collagen and polyAsp resulted in the formation of plate-like crystals. These platelets were 100.9 ± 30.7 nm in length (L), 55.8 ± 9.9 nm in width (W) and 2.9 ± 0.3 nm in thickness (T) (Table 1). The crystals were randomly oriented and evenly distributed throughout the grid (Figure 2A). The diffraction data analysis indicated that the mineral phase in these samples was structurally similar to polycrystalline hydroxyapatite (Figure 2A, inset).

Mineralization experiments in the presence of polyAsp

To better understand the possible mechanism of action of noncollagenous acidic proteins on calcium phosphate precipitation we have used polyAsp as a model polyelectrolyte. We have performed a series of mineralization experiments in the presence of polyAsp at different concentrations. At lower polyAsp concentrations of 3.9 and 7.81 μg/ml, plate-like crystals were observed (Figure 3C,D). The diffraction patterns of these crystals were similar to the control. Though these crystals were similar in shape to that of the control crystals (Figure 2A), average particle dimensions were significantly smaller (Table 1). Specifically, the length of the crystals in the experiments with 3.9 and 7.81 μg/ml of polyAsp were, respectively, 32% and 48% smaller than that in controls (Table 1). A marked difference in morphology and crystallization behavior was observed for crystals obtained in the presence of 15.62 μg/ml polyAsp (Figure 3B). These crystals were much smaller in size (L=47.4± 10.1 nm, W=9.7±2.1 nm and T=2.6 nm) (Table 1), with high aspect ratio of 4.7. The diffraction pattern from this sample was similar

to the controls, although the intensity of the reflections was much weaker. At higher polyAsp concentrations of 62.5 and 125 μg/ml no detectable mineral product was observed.

Mineralization experiments in the presence of collagen

To better understand the effect of collagen on calcium phosphate mineralization we have performed a series of experiments in the presence of collagen fibrils with and without polyAsp.

When the mineralization was carried out on TEM grids coated with a layer of pre-assembled collagen fibrils in the absence of polyAsp, plate-like crystals (L=96.3 ± 25 nm, W=55.5 ± 9.8 nm and T=2.9 ± 04 nm) formed (Figure 2B, Table 2). The size and crystallographic properties of these crystals were similar to the crystals formed in the control experiments (Figure 2A). They were randomly oriented and evenly distributed throughout the grid. No preferred association of the crystals with the collagen fibrils was observed in these experiments (Figure 2B).

The mineralization experiments using grids coated with collagen fibrils in the presence of 62.5 mg/ml of polyAsp have been carried out for 2, 4, and 16 hours as described in the Materials and Methods. As reported above, at this concentration polyAsp inhibits mineral formation. After 2 hours of incubation, TEM analysis revealed arrays of ribbon-like mineral particles deposited within the collagen fibrils (Figure 4). These mineral deposits were observed exclusively in connection with collagen fibrils; no other mineral deposits were observed in the experiments. These ribbon-like mineral particles were preferentially oriented along the fibril. and were 2.8 ± 0.3 nm thick and 68.9 ± 11.2 nm long (Figure 4, Table 2). The width of these particles was impossible to determine reliably, due to the overlap of the crystals inside the collagen fibrils. Interestingly, our, analysis of the mineralized fibrils revealed the diffraction patterns of 8 out of 50 fibrils tested (16%) had only a broad diffraction ring with the d-spacing around 3 Å (Figure 4B, inset), indicating that the mineral particles lack long range crystallographic order, i.e. are amorphous, despite a crystal-like morphology. At the same time a major fraction of mineralized collagen fibrils had typical hydroxyapatite diffraction patterns with distinct (002), (004), (112), (211) and (300) reflections. The 002 and 004 reflections formed distinctive arcs, with an angular spread of ~30° (Figure 4C, inset). The arcs were oriented in the direction of the fibril axis, indicating that *c*-axes of the crystals are co-aligned with the collagen fibril, similar to the situation *in vivo*. It has been reported in the literature that the exposure to the electron beam can trigger transformation of amorphous to crystalline mineral phases [42, 43], it it therefore possible that the actual amount of ACP at this time point is higher. Similarly, after 4 hours of incubation both amorphous and crystalline mineral phases were detected; however only 5% of all fibrils in these samples had amorphous diffraction pattern.

To further asses the evolution of mineral phase additional mineralization experiments were carried out for 16 hour. In this case also, TEM image analysis (Figure 5) revealed bundles of ribbon-like mineral crystals associated with collagen fibrils and oriented with their *c*-axes along the fibrils. The analysis of the diffraction patterns from this sample showed increase in the intensity and narrowing of the angular spread of the 002 and 004 reflections to ~20°, indicating the increase in crystallinity of the mineral as well as the better crystalline alignment. No amorphous mineral has been detected at this data point. At the same time the length and thickness of the mineral particles after 16 hours were not significantly different from the samples incubated for 2 and 4 hours (Table 2).

Hence the results of our mineralization experiments suggest that the interactions of collagen and polyAsp lead to the formation of mineralized fibrils structurally similar to those found in the collagenous mineralized tissues.

We have carried out a series of bio-inspired mineralization experiments *in vitro* with the objectives of better understanding the basic mechanisms of collagen mineralization and furthering the development of bone-like bio-inspired nanocomposites. We were able to recreate the basic building block of CMTs, a mineralized collagen fibril containing stacks of apatitic crystals with their *c*-axes aligned with the long axis of the fibril. Such arrangement of the crystals inside collagen fibrils is the main characteristic of the mineralized collagen fibrils in the CMTs [2, 4, 5].

The data obtained here support earlier observations that collagen fibrils alone do not affect mineralization reaction [15, 44]. At the same time the presence of polyAsp in the mineralization solution triggered mineralization of reconstituted collagen fibrils. Importantly, at the concentrations used in the collagen mineralization experiments, polyAsp alone completely inhibits mineral precipitation and in these experiments the mineralization took place solely in the collagen fibrils. Since, collagen for our experiments was purified from rat tail tendons, which do not mineralize *in vivo*, the probability, that non-collagenous proteins co-purified with collagen could have any effect on the mineralization reaction is very low. These data combined, strongly suggest that the collagen mineralization is induced by polyAsp interacting with collagen fibrils. It has been shown that aspartic acid residues are essential for the specific binding of phosphophoryn and other proteins to collagen molecules [36, 45, 46]. It is therefore feasible that polyAsp preferably binds to specific regions in the collagen fibrils in a way similar to acidic non-collagenous proteins in CMTs and induces the collagen mineralization in its bound form. Similar to polyAsp, A number of acidic noncollagenous proteins have been reported to inhibit mineralization when in solution and induce mineralization when bound to a surface [10].

TEM analysis of the *in vitro* mineralized collagen fibrils reveal parallel arrays of ribbon-like mineral particles aligned with the long axes of the fibrils, similar to the organization of mineralized collagen fibrils *in vivo* [1, 2, 4, 5]. Interestingly, the electron diffraction analysis indicates that a significant fraction of mineral deposited in collagen fibrils in the presence of polyAsp after 2 hours in the experiment lacks a long range crystallographic order, i.e. amorphous. The amount of this amorphous calcium phosphate gradually decreased over time and by 16 hours 100% of the mineral was crystalline. These data suggest that the first mineral phase forming in the fibrils is transient ACP which gradually transforms into an apatitic crystalline phase. Interestingly, these amorphous mineral deposits have ribbon-like shape and organize into parallel arrays along the long axis of the collagen fibrils. The mineral particles transform with time into crystallites without any detectible changes in their morphology. The electron diffraction data indicate that these crystallites are oriented with the c-axes along the long axes of the fibrils. Ten Volde and Frankel [47, 48] have developed a theoretical model of crystalline solids formation via metastable dense liquid phases for macromolecules, which later was expanded to other types of crystallization, including atomic solids [49, 50]. This theory and the supporting experimental data suggest that on the nanoscale crystalline particles do not form via single nucleation event but undergo a series of phase transitions, analogous to the Ostwald's rule, describing mineral phase evolution at the macroscopic level. Mineralization via amorphous mineral precursors has been described in a number of biomineralization systems [20–23, 26, 28], including CMTs [24, 28, 31]. PolyAsp and other polyanions have been previously shown to stabilize amorphous mineral precursors in *in vitro* systems and it has been proposed that acidic biomacromolecules can play a similar role in biomineralization [34, 51–53]. The possible role of ACP in the early stages of CMT mineralization has been suggested decades ago [26]. However, due to challenges of detection of transient amorphous minerals *in situ* it was hard to provide unequivocal evidence of ACP presence at the time. Recently ACP presence along with other metastable transient calcium phosphate phases has been detected in a young bone by Raman micorspectroscopy [24]. Hence, it is quite feasible that the results of our *in vitro* studies replicate *in vivo* mineralization processes in CMTs.

In a recent study Oslzta et al. (2007) [34] describe the mineralization of collagen fibrils in the presence of polyAsp. They propose a mechanism in which polyAsp stabilized ACP initially formed in solution impregnates collagen fibrils and transforms into crystalline mineral. Although, the mineralized collagen fibrils produced in this study are somewhat similar to ours, there are some important differences. Our results indicate that initial mineralization occurs in polyAsp/collagen fibril complex and not in the bulk solution as it is proposed by Oslzta et al. Secondly, in our experiments, the morphology and organization of the particles is determined when mineral phase is still amorphous, whereas Oslza et al. suggest that the amorphous phase homogeneously distributed in and around the fibrils, while the regulation of the shape and organization of mineral particles inside the collagen fibrils takes place during the mineral phase transition and is determined primarily by physical constrains of the collagen fibril. These differences might be due to the variations of the experimental design and additional studies are required to address these inconsistencies.

Our mineralization experiments reveal some unique characteristics of the polyAsp/collagen system. As has been mentioned above polyAsp can affect the shape of the crystals, possibly by the preferred binding to certain mineral faces [54]. In the case of amorphous mineral however it is not clear how this preferred binding can be achieved since amorphous minerals are structurally isotropic. Although the diffused diffraction pattern of the early mineral implies the absence of long range order it is still possible that there is some ordering in the solid, hence some preferred adsorption of the polypeptide might take place. Alternatively, the shape of the particles might be dictated by the physical constrains of a collagen fibril. Another intriguing observation is that the transition from the amorphous to crystalline phase occurs in a controlled manner with the *c*-axes of crystallites co-aligned with the fibril axis. The control of the crystal orientation is typically exerted via template macromolecules that initiate crystal nucleation in solution from a certain crystallographic plane. In the polyAsp/collagen mineralization system first mineral deposits are disordered and the templating mechanism proposed for the classical solution crystal growth is not applicable here. It is possible, especially taking into account the small mineral particle size and their very high surface to bulk ratio, that the collagen or polypeptide on the surface of the amorphous particles can guide their crystallization. A number of literature reports demonstrate that organic templates can initiate amorphous to crystalline phase transition in a controlled manner [21, 55, 56].

The results of our experiment show that polyAsp can play different roles in the calcium phosphate mineralization. Depending on the experimental conditions, it can inhibit mineral deposition, control crystal shape or induce mineralization of collagen fibrils depending on its concentration and either it is surface bound or in solution. PolyAsp is a polyanion with one carboxyl side chain per amino acid and can bind significant amounts of calcium. In sufficient concentrations polyAsp alone can inhibit mineralization in solution by chelating mineral ions and decreasing the free calcium concentration or by binding to crystalline nuclei and faces of growing crystals [13, 54, 57, 58]. At the same time our data suggest that polyAsp can induce mineralization of collagen fibrils, probably by binding to the collagen and creating local Ca^{2+} supersaturation around the fibrils, while simultaneously inhibiting mineral formation in solution. Variety of non-collagenous proteins demonstrate similar plurality of functions dependant on the conditions of the mineralization reactions [10, 59], which might suggest that their functions in CMTs, to a large extent are determined by their polyanionic properties.

Conclussion

In conclusion, we have carried out bio-inspired mineralization of collagen fibrils in the presence of polyAsp as an analog of non-collagenous acidic proteins. Resulting mineralized collagen fibrils closely resemble ones found in CMTs with respect to organization and crystallography. Namely, the mineral crystals in the fibrils were organized into arrays with their c-axes co-

aligned with the long axes of the fibrils. In our experiments the initial mineral particles in the fibrils were crystallographically disordered, however their morphology and organization were identical to the apatitic crystallites found in more mature mineralized fibrils. Our data also indicate that polyAsp influences the mineralization process in a way similar to acidic non-collagenous proteins in bones and dentin. We anticipate that these results will contribute to better understanding of collagen biomineralization and to the development of novel bio-inspired nanostructured materials for tissue repair.

Acknowledgements

The authors are grateful for the financial support provided by NIDCR (NIH) (grant DE016703). We thank the Forsyth Institute Bioimaging Core, Boston, MA and the Center for Biological Imaging at the University of Pittsburgh, Pittsburgh, PA for providing us with the access to TEM. We would like to thank Prof. Prashant N. Kumta for helpful discussions of the results.

REFERENCES

1. Weiner S, Wagner HD. Ann. Rev. Mat. Sci 1998;28:271–298.
2. Landis WJ, Hodgens KJ, Arena J, Song MJ, McEwen BF. Microsc. Res. Tech 1996;33(2):192–202. [PubMed: 8845518]
3. Landis WJ, Song MJ. J. Struct. Biol 1991;107(2):116–127. [PubMed: 1807348]
4. Traub W, Arad T, Weiner S. Proc. Natl. Acad. Sci. U. S. A 1989;86(24):9822–9826. [PubMed: 2602376]
5. Weiner S, Traub W. FASEB J 1992;6(3):879–885. [PubMed: 1740237]
6. Beniash E, Traub W, Veis A, Weiner S. J. Struct. Biol 2000;132(3):212–225. [PubMed: 11243890]
7. Nudelman F, Chen HH, Goldberg HA, Weiner S, Addadi L. Faraday Discuss 2007;136:9–25. [PubMed: 17955800]
8. Addadi L, Weiner S. Angew. Chem. Int. Ed. Engl 1992;31(2):153–169.
9. Weiner, S.; Addadi, L. J. Mater. Chem. 1997. p. 689-702.
10. Boskey AL. J. Cell Biochem 1998:30–31. 83–91. [PubMed: 9513044]
11. Butler WT. Eur. J. Oral Sci 1998;106:204–210. [PubMed: 9541227]
12. Veis, A. Biomineralization. Vol. vol. 54. Washington: Mineralogical Soc America; 2003. Mineralization in organic matrix frameworks; p. 249-289.
13. Goldberg HA, Warner KJ, Li MC, Hunter GK. Connect. Tissue Res 2001;42(1):25–37. [PubMed: 11696986]
14. Hunter GK, Goldberg HA. Biochem. J 1994;302:175–179. [PubMed: 7915111]
15. Saito T, Arsenault AL, Yamauchi M, Kuboki Y, Crenshaw MA. Bone 1997;21(4):305–311. [PubMed: 9315333]
16. Boskey AL, Gadaleta S, Gundberg C, Doty SB, Ducy P, Karsenty G. Bone 1998;23(3):187–196. [PubMed: 9737340]
17. Boskey AL, Spevak L, Paschalis E, Doty SB, McKee MD. Calcif. Tissue Int 2002;71(2):145–154. [PubMed: 12073157]
18. Sreenath T, Thyagarajan T, Hall B, Longenecker G, D'Souza R, Hong S, Wright JT, MacDougall M, Sauk J, Kulkarni AB. J. Biol. Chem 2003;278(27):24874–24880. [PubMed: 12721295]
19. Young MF, Bi YM, Ameye L, Chen XD. Glycoconjugate J 2003;19(4–5):257–262.
20. Addadi L, Raz S, Weiner S. Adv. Mater 2003;15(12):959–970.
21. Beniash E, Aizenberg J, Addadi L, Weiner S. Proc. R. Soc. Lond. B. Biol. Sci 1997;264(1380):461–465.
22. Politi Y, Arad T, Klein E, Weiner S, Addadi L. Science 2004;306(5699):1161–1164. [PubMed: 15539597]
23. Weiss IM, Tuross N, Addadi L, Weiner S. J. Exp. Zool 2002;293(5):478–491. [PubMed: 12486808]
24. Crane NJ, Popescu V, Morris MD, Steenhuis P, Ignelzi MA. Bone 2006;39(3):434–442. [PubMed: 16627026]

25. Lowenstam HA, Weiner S. Science 1985;227(4682):51–53. [PubMed: 17810022]
26. Boskey AL. J. Dent. Res 1997;76(8):1433–1436. [PubMed: 9240379]
27. Termine JD, Posner AS. Science 1966;153(3743):1523–1525. [PubMed: 5917783]
28. Ali SY, Sajdera SW, Anderson HC. Proc. Natl. Acad. Sci. U. S. A 1970;67(3):1513–1520. [PubMed: 5274475]
29. Taylor MG, Simkiss K, Simmons J, Wu LNY, Wuthier RE. Cell. Mol. Life Sci 1998;54(2):196–202. [PubMed: 9539964]
30. Wu LNY, Genge BR, Dunkelberger DG, LeGeros RZ, Concannon B, Wuthier RE. J. Biol. Chem 1997;272(7):4404–4411. [PubMed: 9020163]
31. Anderson HC, Garimella R, Tague SE. Front. Biosci 2005;10:822–837. [PubMed: 15569622]
32. Bradt JH, Mertig M, Teresiak A, Pompe W. Chem. Mater 1999;11(10):2694–2701.
33. Zhang W, Liao SS, Cui FZ. Chem. Mater 2003;15(16):3221–3226.
34. Olszta MJ, Cheng X, Jee SS, Kumar R, Kim Y-Y, Kaufman MJ, Douglas EP, Gower LB. Mat. Sci. Eng. R 2007;58(3–5):77–116.
35. Kuznetsova N, Leikin S. Biophys. J 1999;76(1):A319–A319.
36. Dahl T, Sabsay B, Veis A. J. Struct. Biol 1998;123(2):162–168. [PubMed: 9843670]
37. Miller EJ, Rhodes RK. Methods Enzymol 1982;82:33–64. [PubMed: 7078441]
38. Aoba T, Moreno EC. Calcif. Tissue Int 1987;41(2):86–94. [PubMed: 3115550]
39. Wiesmann HP, Plate U, Zierold K, Hohling HJ. J. Dent. Res 1998;77(8):1654–1657. [PubMed: 9719040]
40. Smith CE. Critical Reviews in Oral Biology & Medicine 1998;9(2):128–161. [PubMed: 9603233]
41. Chapman JA. Connect. Tissue Res 1974;2(2):137–150. [PubMed: 4138005]
42. Beniash E, Addadi L, Weiner S. J. Struct. Biol 1999;125(1):50–62. [PubMed: 10196116]
43. Ziegler A. J. Struct. Biol 1994;112(2):110–116.
44. Hunter GK, Poitras MS, Underhill TM, Grynpas MD, Goldberg HA. J. Biomed. Mater. Res 2001;55(4):496–502. [PubMed: 11288077]
45. Huq NL, Loganathan A, Cross KJ, Chen YY, Johnson NI, Willetts M, Veith PD, Reynolds EC. Arch. Oral Biol 2005;50(9):807–819. [PubMed: 15970211]
46. He G, George A. J. Biol. Chem 2004;279(12):11649–11656. [PubMed: 14699165]
47. ten Wolde PR, Frenkel D. Science 1997;277(5334):1975–1978. [PubMed: 9302288]
48. ten Wolde PR, Frenkel D. PCCP Phys. Chem. Chem. Phys 1999;1(9):2191–2196.
49. Lutsko JF, Nicolis G. Phys. Rev. Lett 2006;96(4)
50. Zhang TH, Liu XY. J. Am. Chem. Soc 2007;129(44):13520–13526. [PubMed: 17929918]
51. Ofir PBY, Govrin-Lippman R, Garti N, Furedi-Milhofer H. Cryst. Growth Des 2004;4(1):177–183.
52. Aizenberg J, Lambert G, Addadi L, Weiner S. Adv. Mater 1996;8(3):222–226.
53. Aizenberg J, Lambert G, Weiner S, Addadi L. J. Am. Chem. Soc 2002;124(1):32–39. [PubMed: 11772059]
54. Burke EM, Guo Y, Colon L, Rahima M, Veis A, Nancollas GH. Colloids and Surfaces B-Biointerfaces 2000;17(1):49–57.
55. Aizenberg J, Muller DA, Grazul JL, Hamann DR. Science 2003;299(5610):1205–1208. [PubMed: 12595685]
56. Xu GF, Yao N, Aksay IA, Groves JT. J. Am. Chem. Soc 1998;120(46):11977–11985.
57. Hoyer JR, Asplin JR, Otvos L. Kidney Int 2001;60(1):77–82. [PubMed: 11422738]
58. Roque J, Molera J, Vendrell-Saz M, Salvado N. J. Cryst. Growth 2004;262(1–4):543–553.
59. Milan AM, Sugars RV, Embery G, Waddington RJ. Eur. J. Oral Sci 2006;114(3):223–231. [PubMed: 16776772]

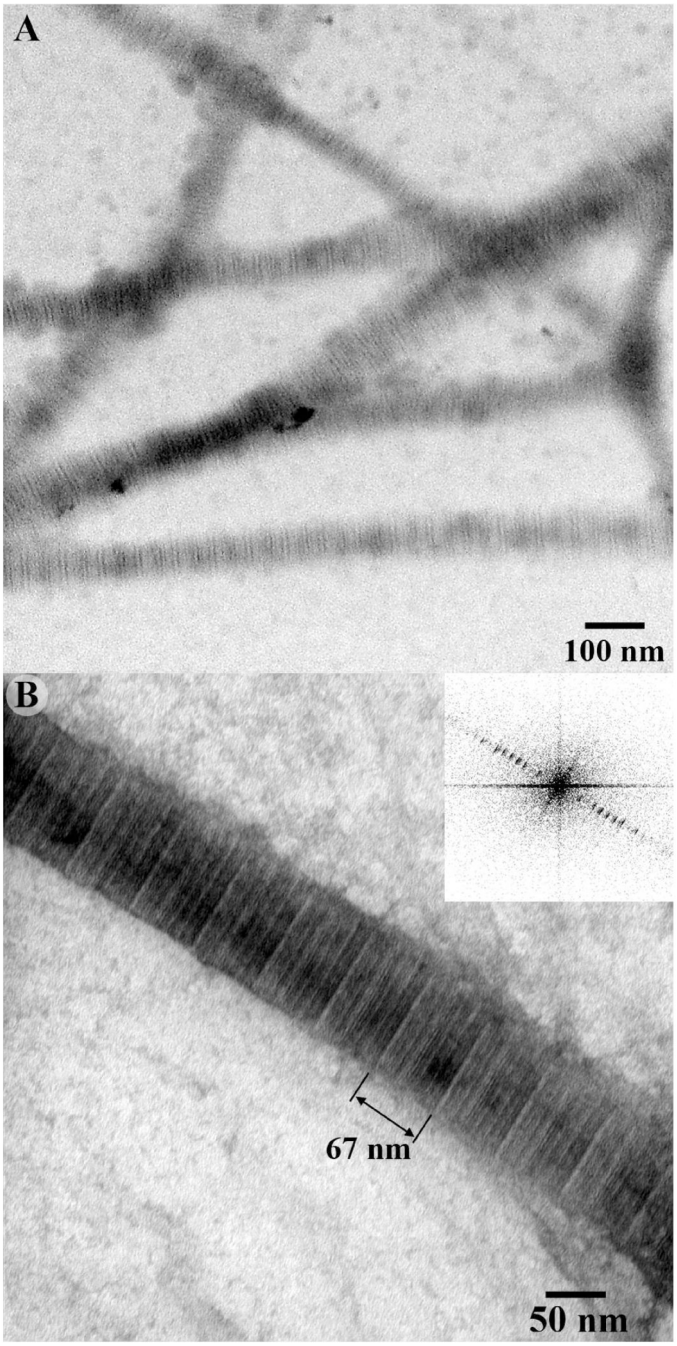

Figure 1.
TEM images of positively stained self-assembled collagen fibril in PBS after incubation at 37° C for 3 hours at low (A) and intermediate magnification (B). The collagen fibrils show typical banding pattern. Based on the Fourier transform data (Figure 1B, inset) the D-spacing of the fibrils is ~67 nm.

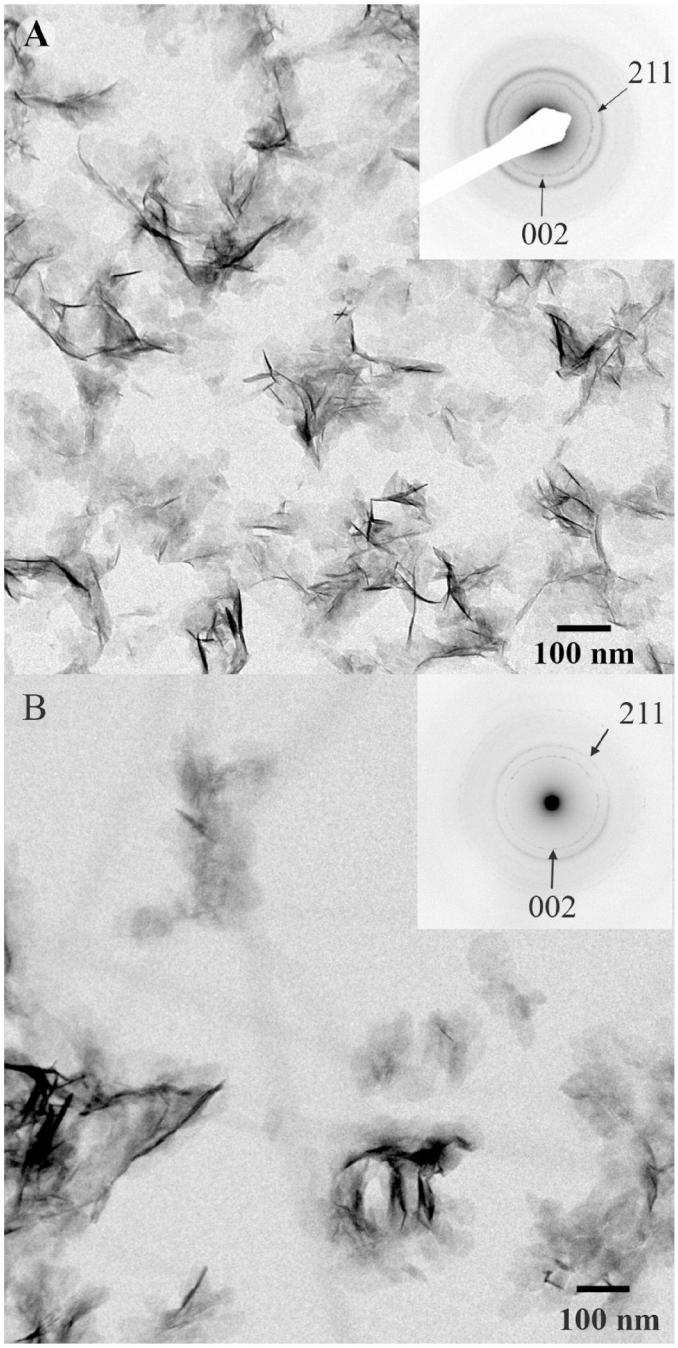

Figure 2.
TEM images of mineral particles obtained by mineralization carried out at 37 °C for 16 hours without polyAsp on (A) bare TEM grid (control) and (B) on TEM grid coated with single layer of collagen fibrils. Corresponding electron diffreaction patterns (insets) show distinct reflection rings with the d-spacings corresponding to 002 and 211 planes of hydroxyapatite.

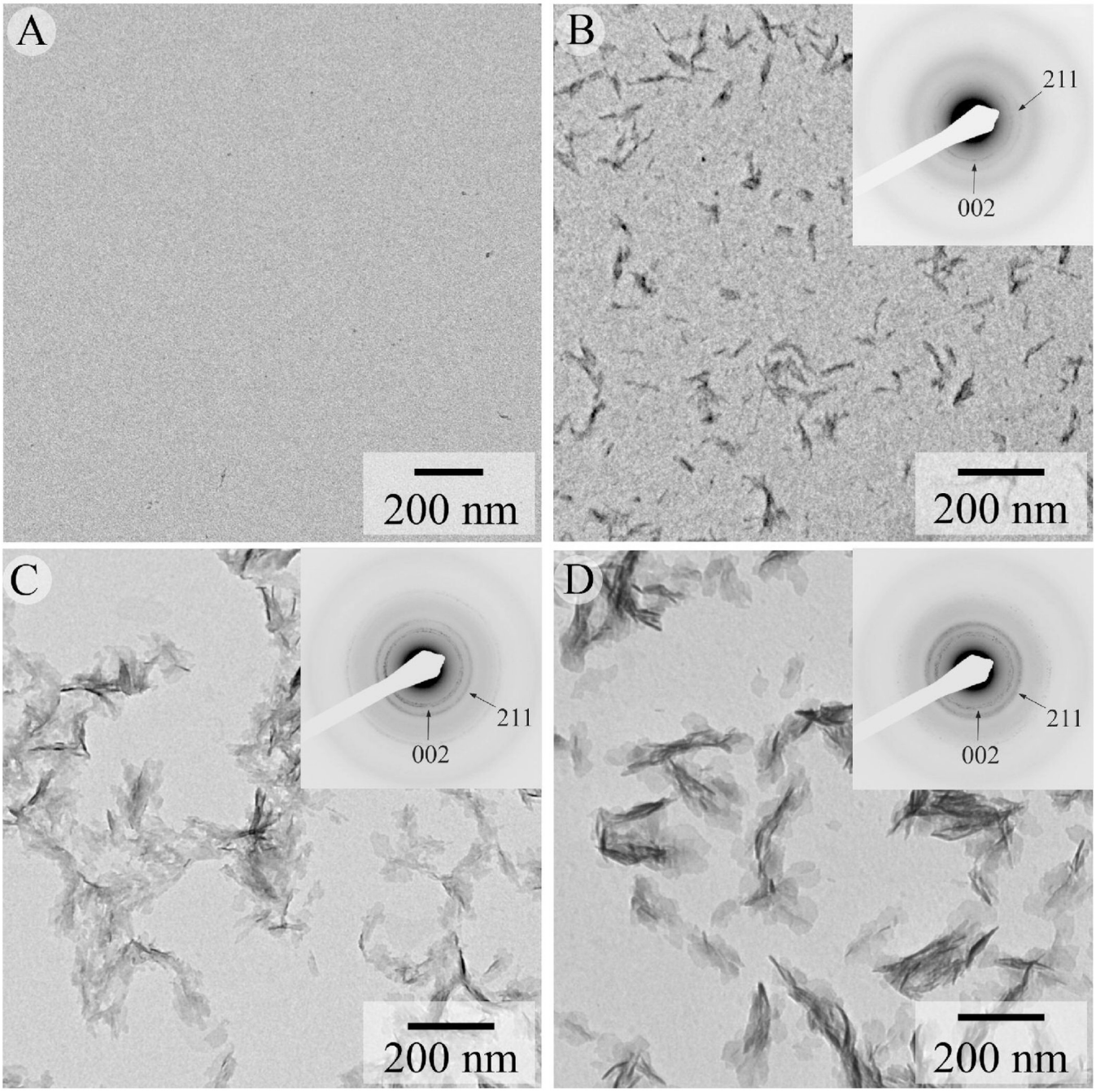

Figure 3.
TEM images from mineralization experiments carried out on bare grids at 37 °C for 6 hours in presence of polyAsp at concentrations of 62.5μg/ml (A), 15.62 μg/ml (B), 7.81 μg/ml (C) and 3.90 μg/ml (D). Corresponding electron diffraction pattern (insets) show reflections corresponding to hydroxyapatite phase. Note the increase in intensity of 002 and 211 reflections with decrease in polyAsp concentration from 15.62 to 7.81 μg/ml.

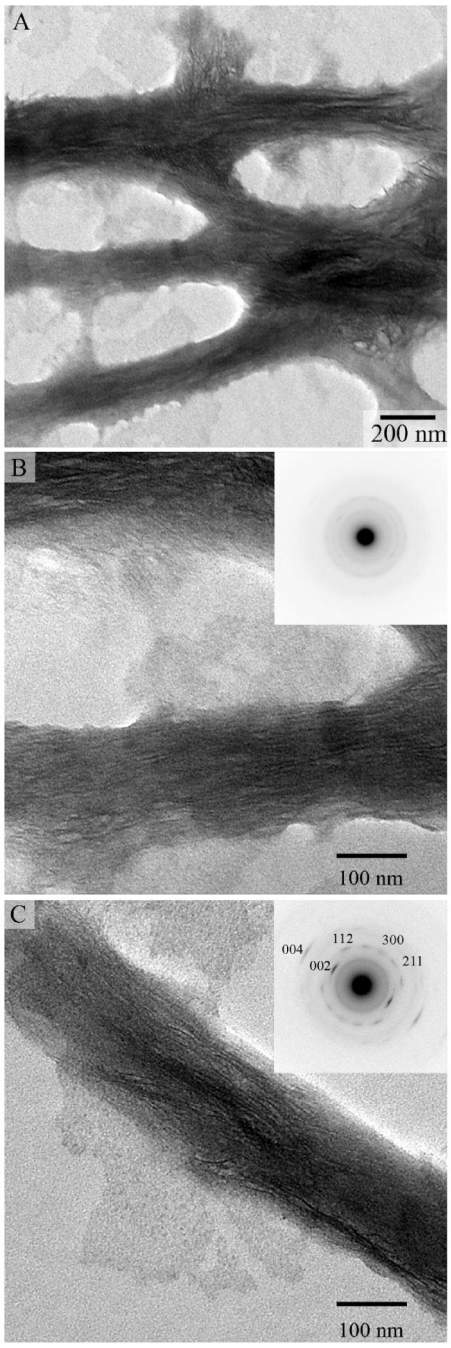

Figure 4.
TEM images and corresponding SAED patterns (insets) of mineralized collagen fibrils incubated for 2 hours. Note the arrays of the ribbon-like mineral particles oriented along the collagen fibril axes. Corresponding diffraction patterns indicate a presence of both amorphous (B) and crystalline mineral phases (C) in the sample.

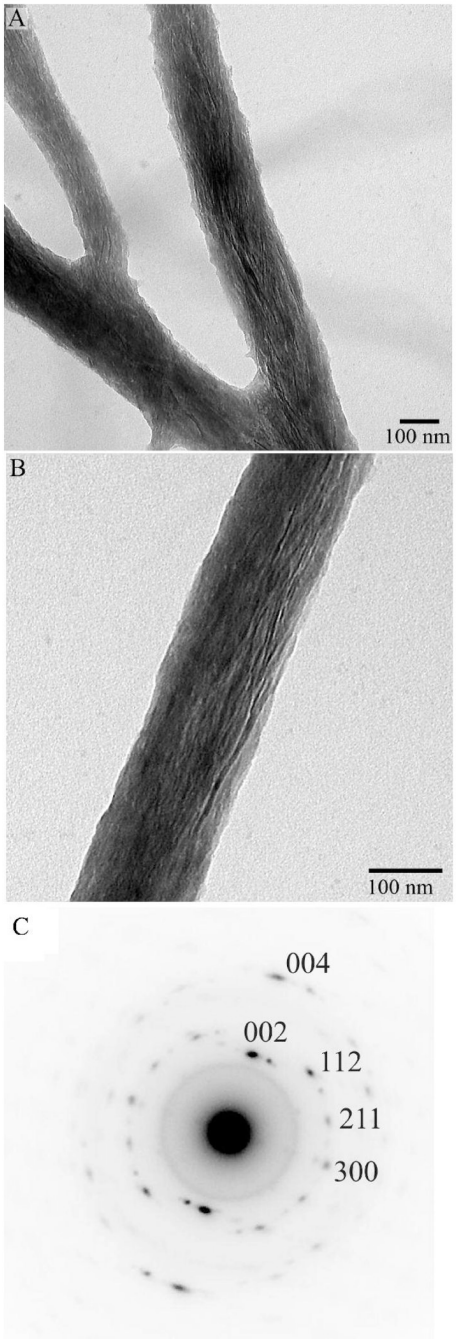

Figure 5.
TEM images of mineralized collagen fibrils for 16 hours at low (A) and intermediate (B) magnifications and (C) the diffraction pattern taken from area in (B).

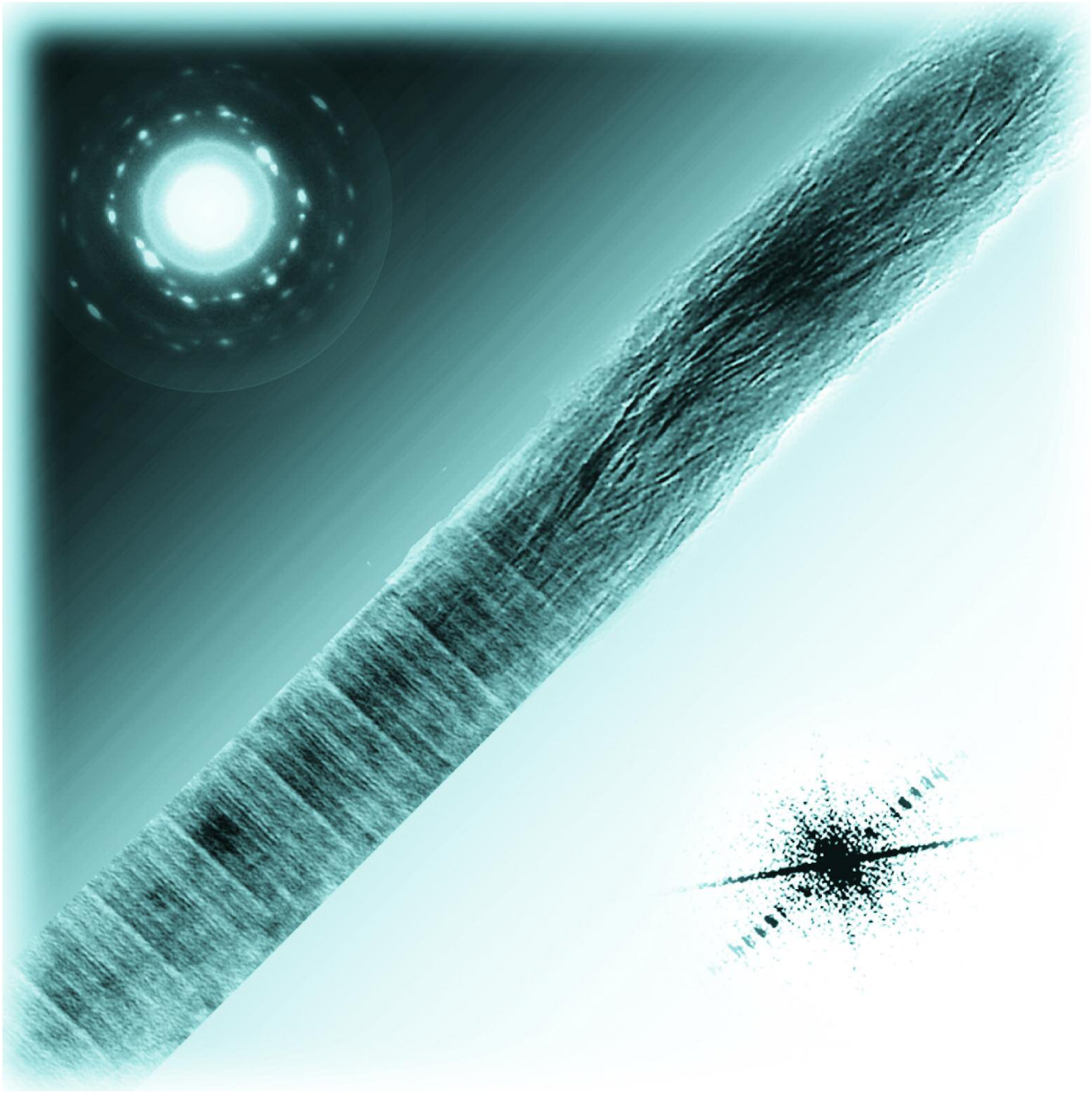

Figure 6.

Table 1

Dimensions of particles formed during mineralization experiments at 37 °C for 6 hours with 1.67 mM Ca2+, 1 mM PO42- and 8.5 mM PBS with systematic variation of polyAsp concentration.

Final concentration of polyAsp (μg/ml)	Thickness[a] (nm)	Length[a] (nm)	Width[a] (nm)
125.00	No mineral formation		
62.50	No mineral formation		
15.62	2.6 ± 0.3	47.4 ± 10.1	9.7 ± 2.1
7.81	2.7 ± 0.3	52.2 ± 10.6	30.3 ± 7.6
3.90	3.0 ± 0.3	67.5 ± 10.6	43.0 ± 11.8
Control	2.9 ± 0.3	100.9 ± 30.7	55.8 ± 9.9

[a] based on 50 measurements

Table 2

Dimensions of mineral particle formed during mineralization experiment with and without polyAsp in presence of collagen at different incubation duration.

Mineralization experiment	Incubation time (hours)	Thickness[a] (nm)	Length[a] (nm)	Width (nm)[a]
Collagen mineralization without polyAsp	16	2.9 ± 0.4	96.3 ± 25.1	55.5 ± 9.8
Collagen mineralization with polyAsp	16	3.0 ± 0.3	73.5 ± 14.5	
	4	2.8 ± 0.3	68.9 ± 11.2	
	2	2.8 ± 0.4	66.9 ± 14.5	

[a] based on 50 measurements